J.M. Pérez, M. Romero. Microstructure and technological properties of porcelain stoneware tiles moulded at different pressures and thicknesses
Ceramics International, 40 (2014) 1365-1377; doi: 10.1016/j.ceramint.2013.07.018

MICROSTRUCTURE AND TECHNOLOGICAL PROPERTIES OF PORCELAIN STONEWARE TILES MOULDED AT DIFFERENT PRESSURES AND THICKNESSES

J.M. Pérez, M. Romero*

Group of Glassy and Ceramic Materials, Instituto de Ciencias de la Construcción Eduardo Torroja, CSIC, C/ Serrano Galvache, 4. 28033 Madrid, Spain

* Corresponding author; E-mail address: mromero@ietcc.csic.es

Abstract

Moulding pressure and thickness are pre-fixed variables in the porcelain stoneware tile industry. This paper examines the effect of both parameters on technological and microstructure properties of unfired and fired porcelain stoneware bodies. The moulding pressure in unfired tiles has a noticeable effect on bending strength and load borne. Common technological properties such as water absorption, porosity, bulk density and bending strength were obtained from the fired tiles. The results indicate that the variation in properties is independent of the thicknesses of the tiles. Moulding pressure affects at lower values, whereas higher moulding pressure produces tiles with similar technological properties. The microstructure exhibits a constant amount of mullite and quartz in all pieces after the firing process. Observations from scanning electron microscopy show that mullite crystals enlarge as moulding pressure increases, but the shape of the crystals are unaffected by the individual thicknesses. Furthermore, the aspect ratio of the mullite needles increases with the moulding pressure, which is invariable to the thicknesses of the tiles. Although the total porosity remains constant, the number of pores is influenced by the thickness. The moulding pressure also influences pore size. The results show a strong relationship between the number of closed pores and the thickness of the ceramic tile.

Keywords: Porcelain Stoneware; Fast-firing; Mullite; Porosity; Density.

1. Introduction

Porcelain stoneware tile is a ceramic material that exhibits superior technical performance in the construction sector. It offers many advantages (lower water absorption and porosity and higher flexural strength) in the design of pavements or coverings compared with other ceramic tiles, such as glazed stoneware. Porcelain stoneware is composed of clay, flux agent and filler. The clay is typically comprised of kaolinite, which confers plasticity to green paste and is the precursor of mullite crystals [1-4]. The fluxing agent is feldspar and the filler is quartz, which most likely lead to higher strengths of the unfired tiles [5-6]. Firing bodies containing these three components exhibit a grain and bond microstructure, which consists of coarse quartz grains joined by a finer bond or matrix that contains mullite crystals and a glassy phase [7].

The variables that govern the industrial process include moulding pressure, firing temperature and soaking time. Data on the last two variables, which have been extensively researched, are reported elsewhere. Regarding moulding pressure, unfired tiles can be shaped by a single- or double-pressing procedure. When single pressing is applied, pressure values in the range of 30–50 MPa are used, which are the values typically presented in the literature [8]. Abadir et al. [9] studied the effects of moulding pressure (35–55 MPa), firing temperature and soaking time in porcelain tiles; however, no previous studies exist in which higher pressures are employed.

Its relatively high density may limit the use of porcelain stoneware in innovative applications, such as for the covering of internal walls or the manufacturing of ventilated facades. Recent studies have reported the manufacture of lightweight porcelain stoneware with reduced densities through the addition of foaming agents, such as CeO2 [10] or SiC [11]. However, the foaming agents cause a reduction in mechanical strength, which limits the maximum attainable reduction in weight. The latest market trends are progressing towards large dimensions (i.e., 60x60 cm2 or 120x60 cm2) and a reduced tile thickness (3–6 mm) [12,13]. However, strong technological limitations constrain the fabrication process. Raimondo et al. [14] examined large-sized ceramic slabs that were manufactured through an innovative ceramic process, including an assemblage of a ceramic fiberglass composite.

Information about the effect of thickness on the technological properties of porcelain stoneware tiles is scarce. The most common technological properties of tiles are assumed unaffected by their thickness; thus, the study of their effect on the microstructure of fired materials has been disregarded.

The present study extends a previous research [8] that concluded that moulding pressure affects the shape of mullite needles, which have a direct effect on the bending strength of porcelain stoneware tiles. The aim of this present study is to expand the previous results by establishing the influence of thickness and moulding pressure on the technological properties and microstructure of typical porcelain stoneware tiles. The microstructural study focuses on the morphology of mullite crystals because the technological properties of the tiles are dependent on the formation of these crystals.

2. Experimental

2.1. Materials and Methods

To obtain the tiles, 50% kaolinitic clay (EuroArce), 40% feldspar (Rio Pirón) and 10% quartz sand were mixed in a planetary mill with distilled water (1:1) for 30 min. Based on the process by Martín-Marquez et al. [15], porcelain stoneware tiles (55 x 15 mm) were moulded in a manual hydraulic press to get four thicknesses (3, 4.5, 6 and 9 mm). Five different moulding pressures (20, 40, 60, 80 and 100 MPa) for each thickness were applied during one minute. Higher moulding pressures were not utilised because Fahrenholtz [16] indicated that moulding pressures above 100 MPa may lead to the development of pressure gradients and other defects that can affect the quality of the tiles after pressing and firing. A specific tile thickness was maintained at different pressures by controlling the quantity of ceramic powder tucked into the mould. The experimental work was divided into two parts: The first part entails the study of the unfired tile properties, such as bulk density and bending strength. The second part entails the microstructural and technological characterisation of the bodies fired at 1200ºC after a fast-firing process , which is similar to the procedure commonly used in industrial manufacturing of porcelain stoneware tiles.

By employing the same procedure described in Perez et al. [8], the bulk density was measured in a hygroscopic balance after weighting the sample in air and immersing it in distillate water.

The bending strength, σf, of 10 test pieces was measured using a three-point loading test in an electronic universal tester (Servosis), with a crosshead speed of 0.1 mm/min for unfired pieces and 1 mm/min for fired pieces (UNE-EN 843-1).

The linear shrinkage, LS (%), of the fired samples was determined by the following equation:

[1]

where Ls and Lc are the length (mm) of the unfired and fired specimens, respectively. The linear shrinkage values of the ten specimens were averaged for each firing temperature.

The determination of water absorption (WA, %), bulk density (BD, g/cm3) and apparent porosity was achieved under conditions found in ASTM C373-88. The test was performed on four representative specimens for each temperature. The unfired samples were measured after protecting them with a waterproof coating (commercial varnish) to avoid the collapse during the experiment.

The open porosity, ε0 (%), total porosity of the sample, εT (%), and closed porosity, εc (%) were measured following the ASTM C329-88 standard.

The microstructure of the fired specimens was examined by field-emission scanning electron microscopy (FESEM) in a Hitachi S-4800 microscope using an acceleration voltage of 20 kV. The porosity of polished surfaces was evaluated using Esprit 1.9 image analysis software. For the analysis of phase assemblages and morphology, fresh fracture surfaces were etched for 4 min in 15% HF solution, washed ultrasonically with distilled water and ethylic alcohol, dried and subsequently coated with Au-Pd in a Balzers SCD 050 sputter. Secondary electron images (SEI) were employed in the microstructure examination.

The mineralogical study were achieved by X-ray diffraction (XRD, Philips X'PERT MPD) operated at 30 mA and 50 kV with Ni-filtered Cu Ka radiation. The phase identification was conducted from the International Centre for Diffraction Data (PDF) (mullite (15-0776) and quartz (46-1045)).

3. Results and discussion

3.1. Unfired tiles

Figure 1a shows the variation in bulk density values as a function of moulding pressure (MP) and thickness (TK). The bulk density of the unfired samples increases as the MP increases with values in the range of 1.64 to 1.90 g/cm3, which corresponds to 20 and 100 MPa, respectively. This variation is due to the difference in the compaction of the unfired tiles. As the MP

increases, the size of the internal pores decreases, and the packing degree increases, which results in higher values of bulk density. The variation in bulk density is not linear. The increase in bulk density with MP is noticeable at lower MPs (from 20 to 60 MPa), but at higher MPs (from 60 to 100 MPa), the tiles exhibit similar bulk density values. Nevertheless, bulk density is nearly unaffected by the TK of the tiles. For a specific pressure, the thicknesses of the tiles only changes when there is a proportional adjustment of the mass. However, at low pressure (20 MPa), an increase in thickness from 3 to 9 mm yields a variation of 8% in the bulk density. Figure 1a also shows the variation in density of the unfired tiles reported by Pérez et al. [8]. The values depict a similar trend. The curve is displaced towards higher density values, which is most likely due to the greater compactness of the bodies obtained by the automatic pressing process; this process is dissimilar to the manual pressing step that was employed in the present study.

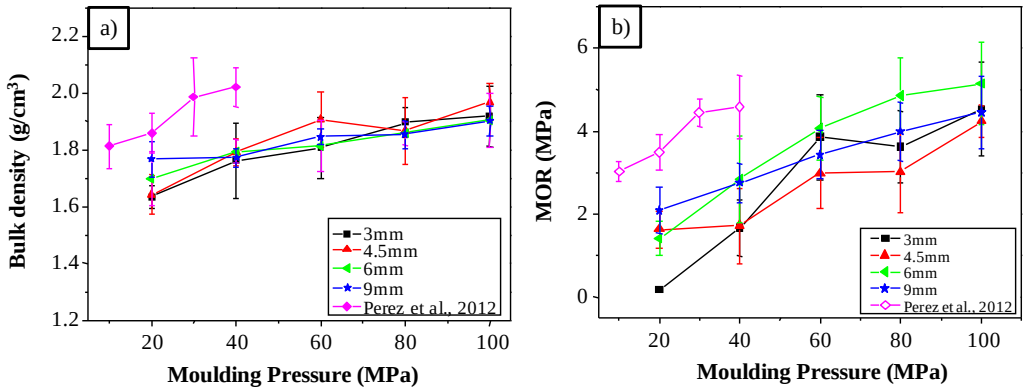

Figure 1. a) Bulk density of unfired tiles shaped at different moulding pressures and thicknesses; b) Variation of bending strength of unfired tiles with moulding pressure. (both straight and dotted lines drawn in Figs. 1 to 4, 6 to 9 and 12 are included for visual guidance).

Figure 1b depicts the variation in bending strength of the unfired tiles as a function of MP and TK. In all cases, the modulus of rupture (MOR) is higher than 0.1 MPa, which is the minimum value that enables unfired bodies to extract the tiles from the die and transport them along the manufacturing line. As expected, the lowest MOR value (0.19 MPa) corresponds to the tile shaped at the lowest thickness and lowest pressure (3 mm and 20 MPa, respectively), and the overall trend progresses to higher MOR values as the MP increases, which is in agreement with the previous results [8]. The effect of MP can be verified by the difference in σf values that correspond to the tiles moulded to the lowest pressure and the highest pressure, which are 20

and 100 MPa, respectively. Note that the resistance increases with pressure, which is a reasonable result considering that increased pressure leads to higher compaction as illustrated in Fig. 1a. However, this variation is non-linear because the greatest differences are observed between 20 and 60 MPa for all thicknesses. These results confirm the existence of a threshold in MP, above which the increment of MP produces a slight variation in σf.

3.2. Fired bodies

Once the unfired tiles were subjected to a fast-firing cycle, the fired products were examined to establish their technological properties (linear shrinkage, water absorption, porosity and bending strength), microstructure and phase composition. Figure 2 shows the variation of LS and WA after the fast-firing processing of the bodies, which were moulded at different pressures and thicknesses. Lower shaping pressures (20, 40 and 60 MPa) have an important effect on LS (Fig. 2a) of thinner tiles (3 and 4.5 mm). The porosity of unfired compacts that were pressed at low pressure is relatively high, as indicated by the difference in the bulk density values (Fig. 1a). In liquid-phase sintering, the wetting liquid acts on the solid particles to eliminate porosity and reduce interfacial energy, as higher-energy solid-vapour interfaces are gradually replaced by lower-energy solid-solid interfaces with a total decrease in free energy occurring on sintering. Consequently, shrinkage of the fired body decreases as the unfired density of the compact increases. The greatest variations in shrinkage occur in the samples pressed from 20 to 60 MPa; however, this difference is almost negligible in bodies pressed from 60 to 100 MPa.

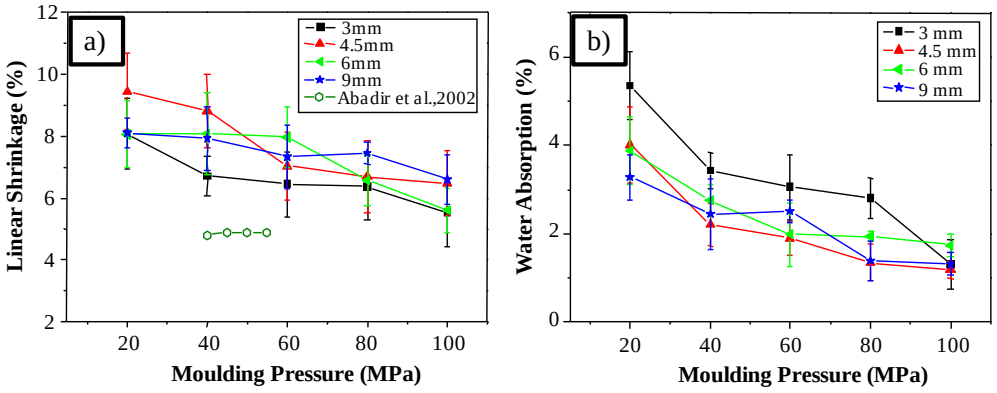

Figure 2. a) Linear shrinkage and b) water absorption of the fired bodies. Empty hexagons data are from Abadir et al.[9]

According to Amorós [17] the compaction of a granular material occurs through three stages: Stage I (initial), which extends from the start of the compaction up to the granule flow pressure (Pf), in which the granules reach the maximum degree of compaction without the occurrence of deformation or destruction. The Stage II (intermediate) comprises the pressure range that extends from Pf up to the pressure value at which the density of the body matches the granule density. The greater part of the compaction occurring in the body during the pressing process occurs at this stage, by deformation and/or destruction of the granules. Throughout the Stage II, practically all the reduction of the porosity is due to the elimination of inter-granular porosity; finally, at Stage III (final) the increased compaction of the body results from the elimination of intra-granular porosity by rearrangement of particles. Therefore, in the 20-60 MPa pressure interval, the ceramic body would be in an intermediate state of compaction, in which the reduction in both volume and size of inter-granular spaces takes place by plastic deformation. In this state, a slight increase in pressure results in a notable increase in the degree of compaction as consequence of removing the inter-granular porosity, whereas intra-granular porosity remains unchanged. In the 60-100 MPa pressure interval, the ceramic body is in the final state of compaction, in which the reduction in volume and size of intra-granular pores takes place. In this state, a large increase in pressure leads to negligible changes in compaction.

The LS results reported by Abadir et al. [9] concluded that increasing the MP above 45 MPa did not enhance the sintering degree of fired tiles (Fig. 2a), whereas the results showed in the present study indicate that in the pressure range considered, LS tends to decrease with an increase in MP.

Figure 2b) reveals that WA decreases as MP increases, due to the higher densification of tiles. The WA of compacts pressed at 20 MPa and 40 MPa exhibit higher differences, whereas the variations observed are much lower for MP above 40 MPa. This finding is in agreement with the LS results, i.e., there is less space between particles, which indicates that fewer pores remain. Therefore, as the MP increases, the capability of WA decreases. Concerning tile thickness, the thinnest tiles exhibit the highest WA values. However, WA is independent of thickness for the other tiles. The WA values from porcelain stoneware tiles presented in this study are higher than typical values. This result can be attributed to the initial mixture of raw materials, which includes high amount of clay and low amount of feldspar and favours mullite development. Therefore, the selected composition produces fired bodies with higher porosity and, hence, higher WA values.

Figure 3 depicts the effect of densification on the bending strength of fired tiles. It can be seen that MOR values of fired tiles are independent of TK. However, as bulk density of fired tiles increases, their final strength also improves. Thus, an increment of 9% in BD leads to an increase of 57% in MOR results. This result implies that the final mechanical properties are highly affected by densification.

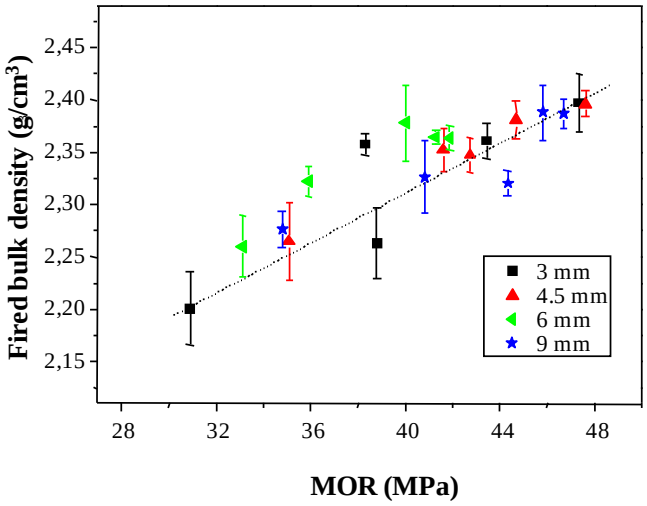

Figure 3. Fired bulk density variation with MOR.

Figure 4 depicts the variation of open, closed and total porosity (ε0, εc and εT, respectively). The greatest variation in open porosity is observed between samples shaped at 20 and 40 MPa, as a consequence of the lower compactness exhibited by unfired tiles pressed at 20 MPa. A low density prior to firing implies a high volume of voids that need to be eliminated and, consequently, the remaining open porosity after firing will be higher (≈14%). These results are in agreement with Amorós et al. [18], who showed that the presence of large pores in the unfired tiles inhibits the densification process and requires higher firing temperatures to achieve the maximum densification of the product. These results are also in agreement with previous WA results (Fig. 2b). Conversely, closed porosity also exhibits a significant decrease as the MP increases to a maximum of 40 MPa, whereas closed porosity increases at higher pressures owing to the pressure exerted by the gas entrapped in the closed pores, which causes an increase of the pore size [19]. However, other factors such as pore coarsening and change in the amount and viscosity of vitreous phase are also affecting to the development of close porosity [20]. Note that at the first stage of sintering, a high compactness locks the microstructure and inhibits the rearrangement of particles [21]. Overall, the total porosity of fired tiles noticeably decreases

from 20 to 40 MPa and afterwards slightly increases. In general, the variation in porosity is similar to the variation showed in literature [8], in which small differences may have resulted from the change in firing temperature (80ºC lower in the present study). Furthermore, the results shown in Fig. 4 are similar to the results found in the literature (tiles fired at 1260ºC, which yield εT = 13%) [22]. Figure 4d shows a clear effect of total porosity over MOR. Lower porosity of fired tiles gives higher values of bending strength. In fact, a decrease of 8% in total porosity produces an increase of 34% in MOR [23-25].

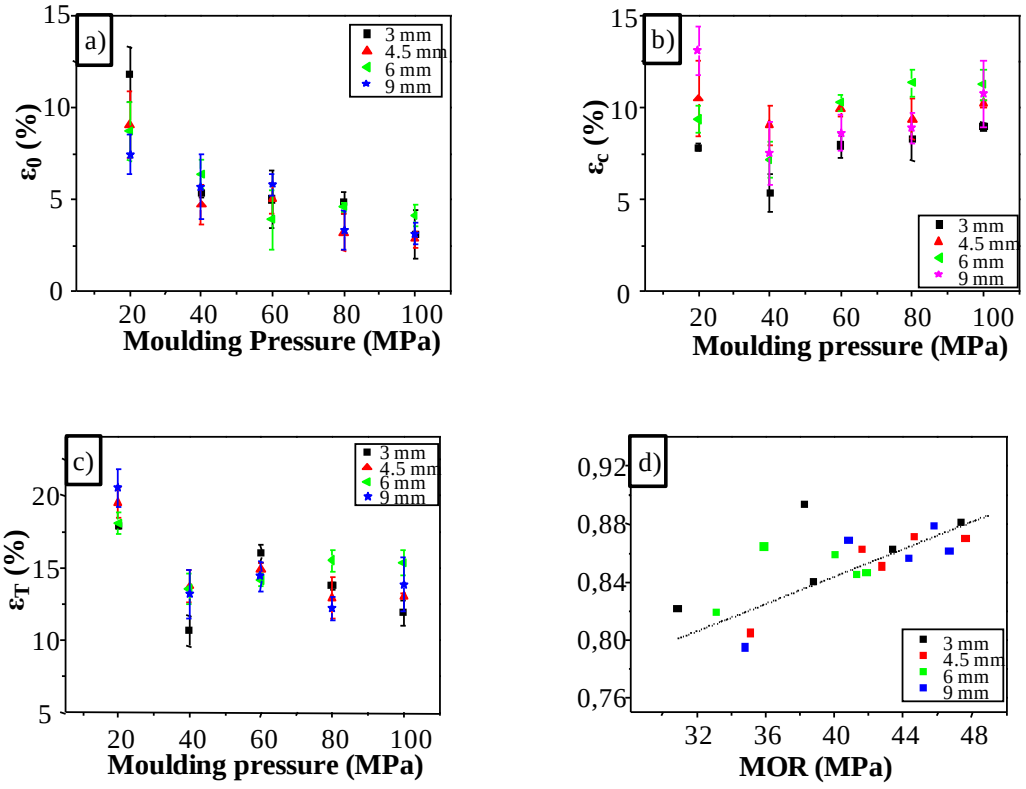

Figure 4. Variation of a) open (εo), b) closed (εc) and c) total (εT) porosity with MP; and d) 1-εT with MOR of fast-fired stoneware tiles.

These results indicate that the differences in the properties obtained with pressures above 60 MPa are generally negligible for total porosity and linear shrinkage.

Figure 5 shows the internal microstructure of fired porcelain stoneware that is shaped at two moulding pressures (40 and 80 MPa) and four thicknesses (3, 4.5, 6 and 9 mm). The SEM micrographs show the existence of both open and closed porosity after firing. Typically, open porosity consists of fine and interconnected pores with irregular shapes, whereas closed porosity

consists of larger, isolated and spherical pores. Figure 5 demonstrates that open porosity generally decreases as MP increases; this reduction is more noticeable at lower TKs. A higher MP leads to highly compact unfired bodies with a lower volume of voids; therefore, the elimination of open pores by the liquid phase formed during firing is favoured. As the TK and MP increase, the number of closed pores decreases. Nevertheless, it is a visual appreciation due to the difficulty of assessing two variables (pressure and thickness) that simultaneously affect porosity.

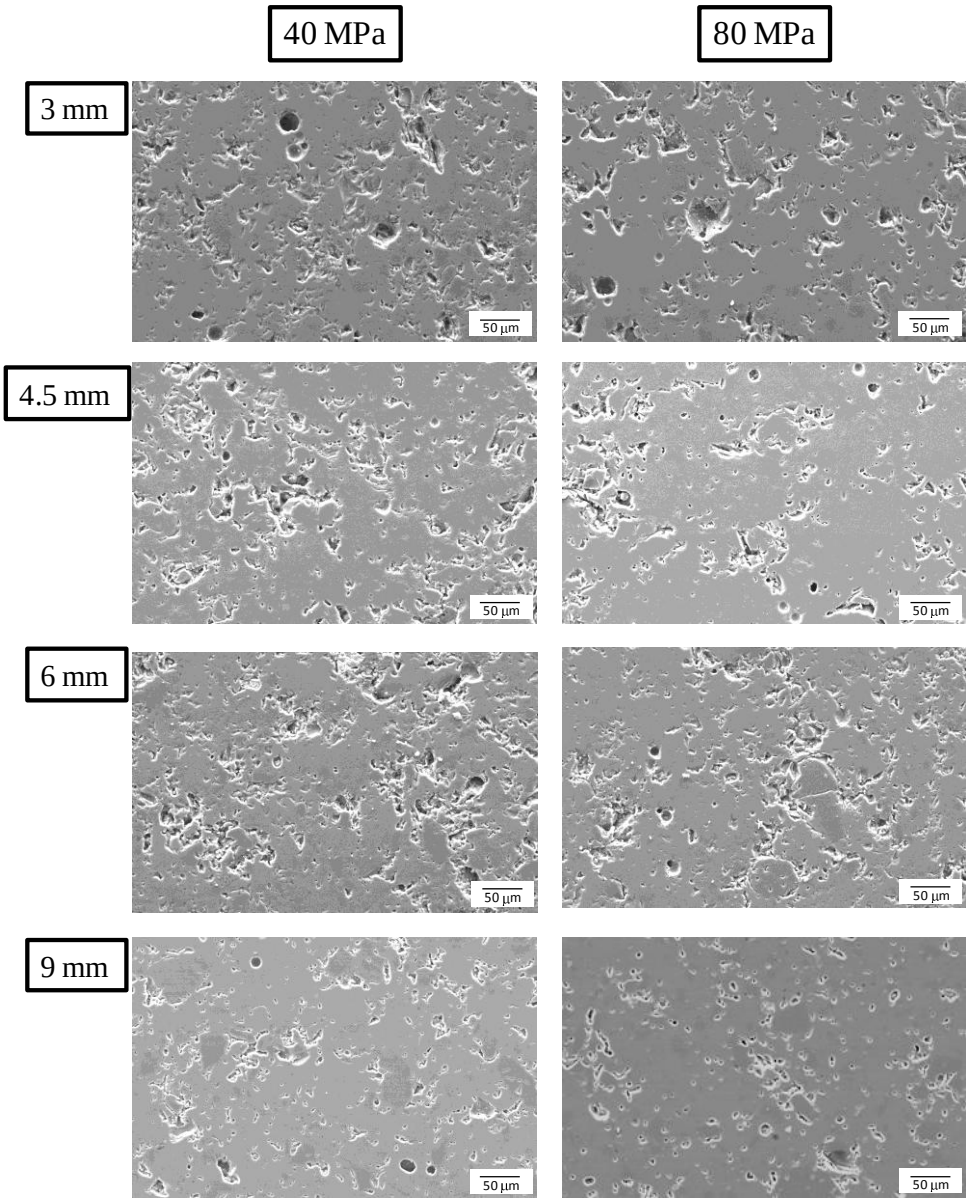

Figure 5. SEM micrographs on the polished surfaces of the fired porcelain stoneware shaped at 40 and 80 MPa.

For a better evaluation, Figure 6 displays the number of closed pores per mm2 determined from eight micrographs for each type of tile. Note the strong relationship between the number of closed pores and the tile thickness; the number of pores increases with the TK of the tile. This result is most likely due to the temperature gradient inside the tile during the firing cycle. This gradient is expected to increase as the TK increases, which leads to differences in the liquid phase viscosity from the surface to the core of the tiles. Thus, as the thickness increases, the viscosity in the core of the tile will increase, which inhibits the removal of voids. Therefore, the fired product exhibits a greater number of pores. Regarding the MP, the number of pores is observed to increase at a higher MP, which is more significant for the thickest tiles (6 and 9 mm). At higher shaping pressures, there is greater contact between the particles in the unfired tiles, which causes a greater number of smaller voids and, as previously explained, the elimination of theses pores is restrained in the thickest tiles.

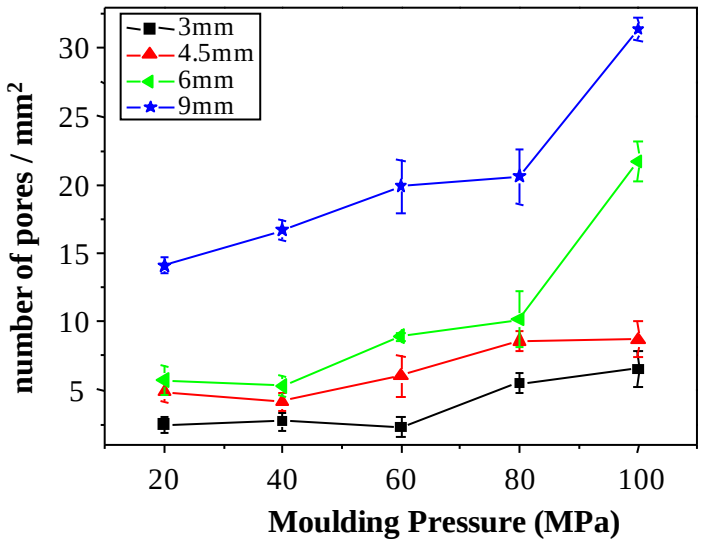

Figure 6. Pores density obtained from SEM micrographs of the fired tiles.

Gil et al. established [26] that closed pores with sizes lower than 5 μm are caused by irregular porosity, which has been progressively closed during the sintering process. Lager pores, whose sizes exceed 10 μm, constitute coarse closed porosity. These pores are produced in regions with fluxing and are related to stain resistance.

Figure 7 depicts the cumulative curves of pore-size distribution for different MPs. To better understand the effect of TK and MP on both number and size of closed pores, the pore size has

been divided into different ranges. The analysis shown in Fig. 7 demonstrates that the size of the closed pores is related to tile thickness. Hence, the thinnest tiles contain a significant percentage of large-sized pores (there are few pores of lower sizes), whereas the thickest tiles contain a significant proportion of smaller-sized pores (curves shows that 50% is reached with lower pores range). From the data, the maximum percentage of pores for 3 mm tiles is in the range of 20–30 μm (40 MPa), but the maximum percentage for 9 mm tiles is in the range of 0–5 μm (40 MPa). The remaining tiles shaped at different MP exhibit a similar tendency. In uniaxial pressing, the friction between the particles and between these and the walls of the mould causes an heterogeneous distribution of the compression pressure through the volume of the ceramic body, which causes the existence of density gradients in the shaped tiles [27]. Thus, the mean axial pressure acting on a plane parallel to the application of the load and located at a distance z decreases exponentially as the distance z increases [28]. Consequently, at the same shaping pressure the pore size decreases as the thickness of the tile increases.

Figure 8 shows the effect of MP and TK on the bending strength of fired tiles. As the MP increases, the MOR increases from 30 to 47 MPa. There is a disparity between the current and previous results for the unfired tiles due to the shaping process, whereas such variance is nonexistent for the fired tiles. This finding indicates that the differences in the physical properties of the unfired bodies, which were derived by the shaping process, can be overcome by the firing process. Conversely, the MOR is less dependent on the thicknesses of the fired tiles compared with the MOR of the unfired tiles. As previously stated, the compactness is the predominant factor affecting the bending strength of the unfired bodies; as fewer pores exist, the space contributing to fracture is lower. Open porosity has an effect on the bending strength in fired tiles [29] and, thus, the lower porosities (Fig. 4a) imply higher MOR values. Other factors also affect bending strength, such as mullite formation and quartz particles [1-3,30,31], which will be considered subsequently. From Figs. 6 and 7, it can be deduced that a higher MP implies a maximum number of lower-sized pores for 9 mm tile and, thus, numerous small pores help the tile to bear higher loads than fewer large pores. However, for a specific MP, the improvement in resistance is lower as TK increases (i.e., 20 MPa: between 3 and 6 mm, there is an increase of approximately 230% in the strength value, whereas the increase in the strength value is approximately 120% between 6 and 9 mm).

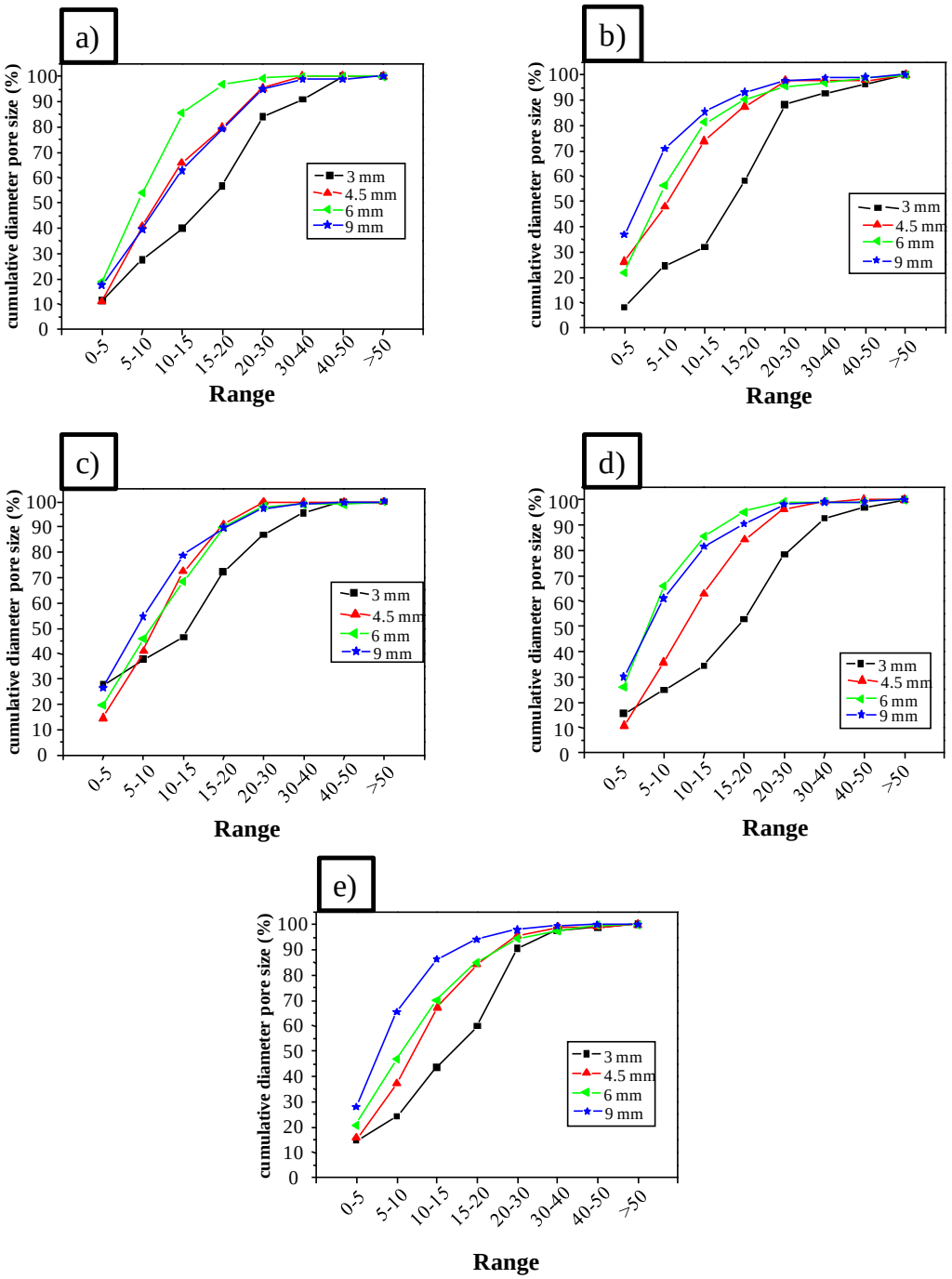

Figure 7. Cumulative curves of pore sizes as a function of the thicknesses of the fired bodies shaped at a) 20 MPa, b) 40 MPa, c) 60 MPa, d) 80 MPa and e) 100 MPa.

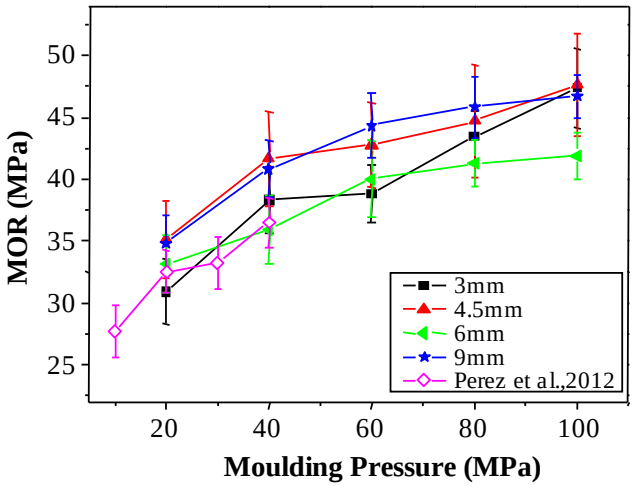

Figure 8. Bending strength of the fired tiles as a function of moulding pressure and thickness.

Figure 9 displays the X-ray diffractograms of the fired porcelain bodies, which are composed of mullite and quartz. These results confirm that the amount of mullite formed on firing is only dependent on the percentage of clay, temperature and firing time, but is not dependent on the MP or the TK. The intensity of X-ray peaks shows negligible variations, as displayed in the box at the top of Fig. 9 [32].

Figure 10a shows the microstructure of fired porcelain stoneware samples moulded at 3 mm and 100 MPa. The fine cuboidal crystals correspond to Type I primary mullite (M-I), which are developed from pure clay agglomerate relicts. Further growth of these crystals results in elongated needle-shaped crystals of secondary mullite, which were formed in regions in which feldspar particles were well mixed with kaolinitic clay or where feldspar moved through clay agglomerates [33]. Both cuboidal and needles mullite crystals are common in all fired samples, which demonstrates the greater differences in shape and size of the secondary mullite needles that were grown in tiles moulded at different MP. Figure 10b details the morphology of secondary mullite, which was developed in 3 mm tiles shaped at the lowest pressure (20 MPa). These tiles yield needle-like crystals that are ~3.2–4.6 μm long and ~0.1 μm wide, which correspond to a mean aspect ratio of 30:1. By considering the notation accepted in the literature [7], these crystals can be considered secondary Type II mullite.

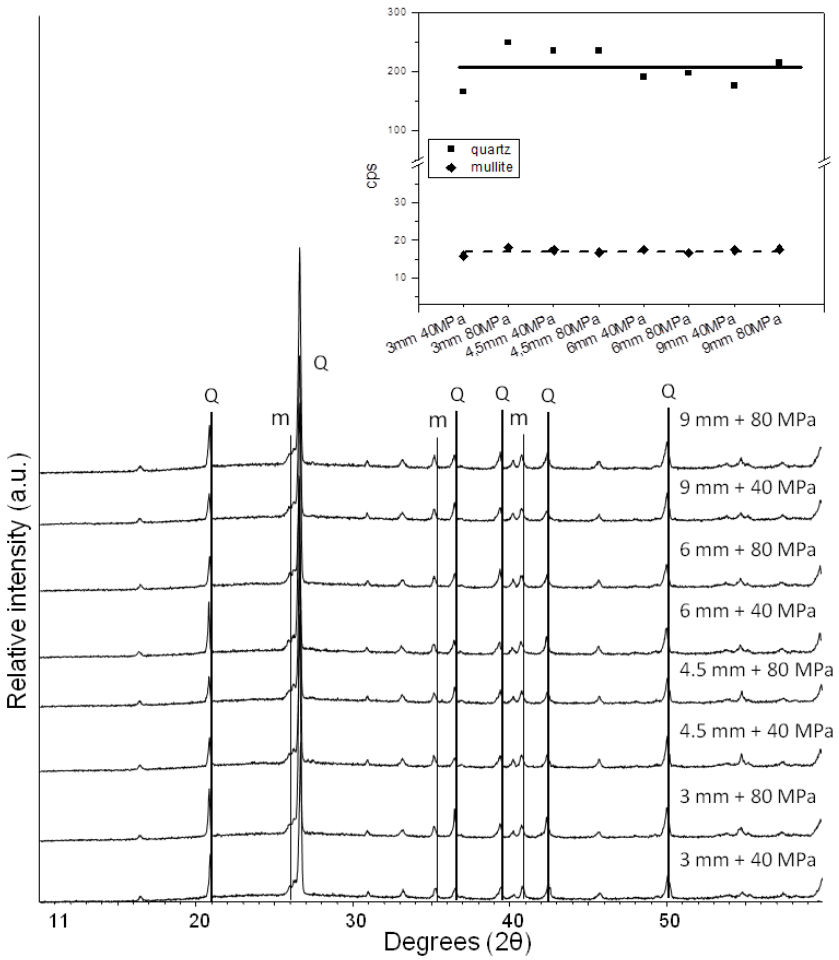

Figure 9. X-ray diffractograms of the fired porcelain bodies shaped at 40 and 80 MPa. The top box represents the variation in the intensity of quartz (2θ = 26.5º) and mullite (2θ = 60.6º) peaks.

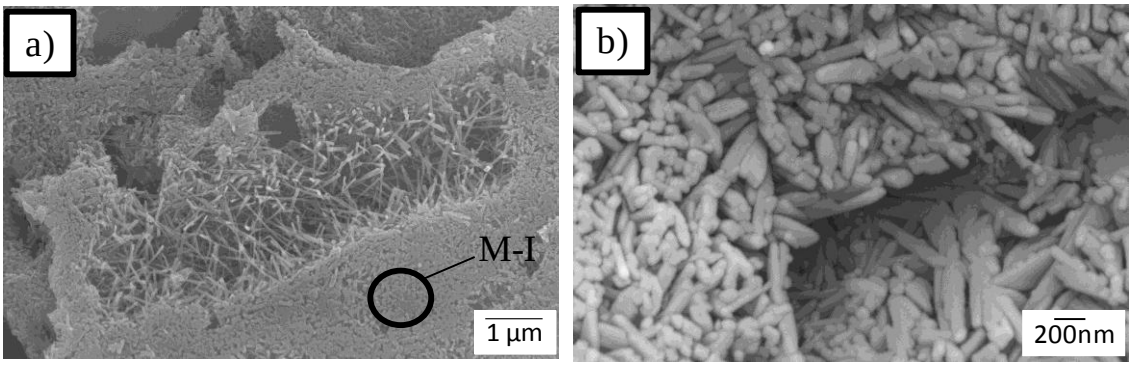

Figure 10. SEM micrograph of the 3 mm thick porcelain stoneware shaped at a) 100 MPa and b) 20 MPa.

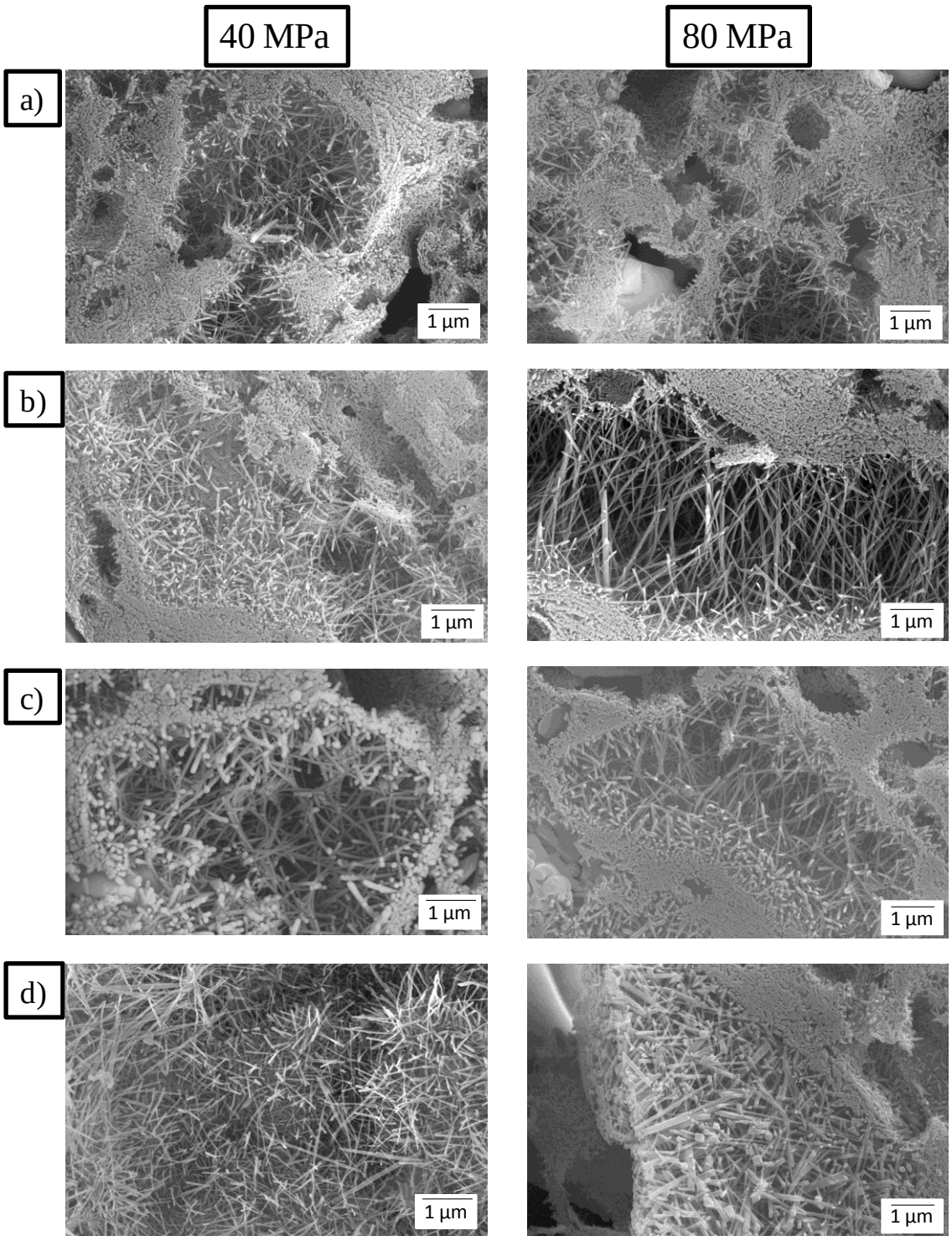

Figure 11. SEM micrographs of fresh-fractured fired tiles shaped at 40 and 80 MPa: a) 3 mm, b) 4.5 mm, c) 6 mm and d) 9 mm.

It is widely accepted that the development of Types II and III secondary mullite during the firing of porcelain stoneware tiles is assisted by the liquid phase, which is formed from the melting of the feldspar component and partial dissolution of quartz particles. Figure 9 presents the negligible effect of MP on the percentage of amorphous and crystalline phases after firing. Therefore, the mullite crystals developed during firing must be surrounded by a similar amount of liquid phase that should also exhibit comparable viscosity, as all samples have the same batch composition and firing schedule. Thus, the differences observed in the aspect ratio of mullite needles in samples moulded at different pressure must be related to the arrangement of mullite crystals and liquid phase during firing, that is, to the contact degree between both phases. This result agrees with those studies8,9 on porcelain stoneware moulded at lower MP.

Two recent studies [8,31] have demonstrated that bending strength in porcelain stoneware is directly associated to the aspect ratio of secondary mullite needles. As illustrated in Fig. 6, bending strength increases with MP, which also leads to higher aspect ratios of mullite needles. Figure 12 depicts the variation in bending strength as a function of the aspect ratio, which is shown by the secondary mullite needles developed in samples at different MP and TK. As mentioned previously, the aspect ratio of the secondary mullite needles is independent of the TK. In contrast, the MP has a marked effect on the aspect ratio, and the bending strength improves when the aspect ratio increases from 29:1 in samples pressured at 20 MPa to 62:1 in samples pressured at 100 MPa. The results presented in Fig. 12 are compared with Martín-Márquez el al. [31] and Perez et al. [8]. The curves fit together, which demonstrates the direct association of both factors (mullite shape and bending strength). This result is consistent with the mullite hypothesis as a mechanism to strengthen, which establishes that the strength of a porcelain body is related to the interlocking of fine mullite needles [23,34].

However, the aspect ratio of the mullite crystals is not the only factor that affects the flexural strength. As discussed in Figure 3, the value of MOR increases with increasing density of the fired piece, which is governed by the microstructure of the matrix, consisting of quartz and mullite microcrystals and the glass phase. In this sense, Zanelli et al. [35] suggest that this matrix is the real "viscous phase", which regulates the kinetics of densification in the course of firing of porcelain stoneware tiles. Recently, de Noni et al. [36] demonstrated that the positive effect of mullite needles on mechanical properties is clearly manifested with a high the cooling rate at the final stage of the firing process, as the case of the present study in which the tiles have been fired following a fast-firing schedule

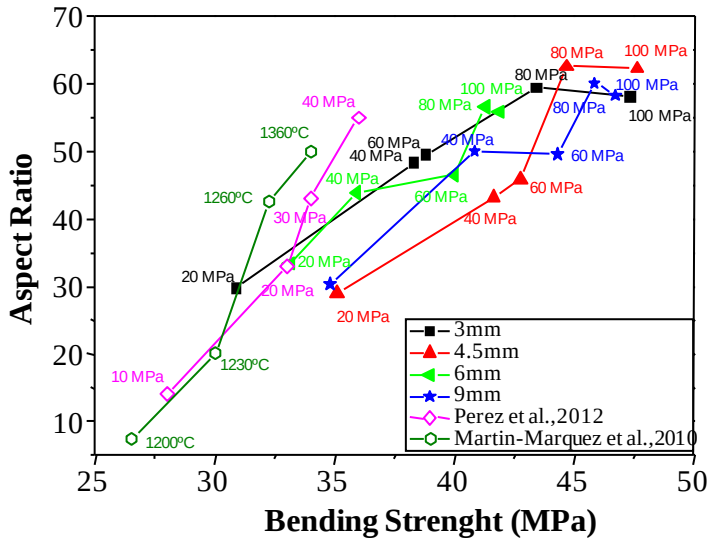

Figure 12. Variation in bending strength as a function of the aspect ratio of the secondary mullite needles. Empty points are values from Perez et al.8 and Martín-Márquez et al.[24]

Figure 13 details the microstructure of secondary mullite needles that were developed in the 4.5 and 9 mm tiles moulded at 80 MPa. Regardless of their TK, most of the tiles shaped at high MP exhibit Type III mullite needles, which reveal an internal hole along their longitudinal axis. This morphology has been described previously in the literature [8,37], in which "clusters or packs of needles" is used to describe Type III mullite. When a cluster of mullite needles is formed, more than two needles combine forming one new thicker needle. This new cluster may form from the junction of several needles that rapidly join together without allowing the liquid phase to recede; thus, the liquid phase remains inside the cluster.

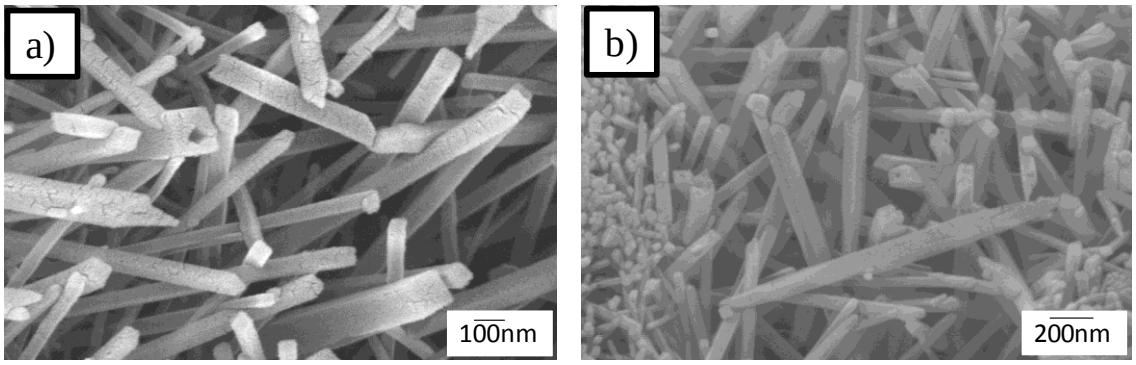

Figure 13. SEM micrograph of fired porcelain stoneware tiles shaped at 80 MPa with thicknesses of a) 4.5 mm and b) 9 mm.

Figure 14 displays the microstructure of fired porcelain stoneware samples shaped at the lowest and highest MP (20 and 100 MPa), in which two new types of mullite clusters have been found. Although these clusters are less distinct in the thinnest tiles, they are very noticeable in the remaining TKs. Thus, in tiles shaped at 20 MPa the clusters may be described as a mixture of secondary mullite needles joined with numerous primary mullite flakes. These clusters may be mainly attributed to decreased contact among the particles due to the low MP. Conversely, another type of mullite cluster was discovered at the highest MP (100 MPa), which is similar to the mullite clusters mentioned in Fig. 13 and in the literature [8,37]. However, their shape differs from previously reported results. They now appear as "unfinished clusters", i.e., the secondary Type III mullite needles have joined but a deterrent prevents these needles from forming final clusters, which is similar to the clusters presented in Fig. 13. This impediment may derive from the greater compactness of tiles pressed at the highest MP, creating smaller voids between the clay and feldspar particles and, thus, a different growth of clusters.

Apart from the above-mentioned clusters, the micrographs in Fig. 14c and d illustrate that well-defined "prismatic" particles also form at 100 MPa, which were detected in nearly all samples regardless of their MP or TK. In higher MP tiles, these particles are more abundant than in lower MP tiles. Figure 15 presents additional micrographs that show prismatic particles. Although prismatic particles can be mistaken for external particles that could have been added during sample preparation (because of the fracture process), an ulterior EDX analysis (not shown here) has shown that those prismatic particles correspond to mullite ($3Al_2O_3{\cdot}2SiO_2$) despite the appearance of particles over the fracture surface of the tiles. This morphology of mullite crystals has not yet been described for porcelain stoneware.

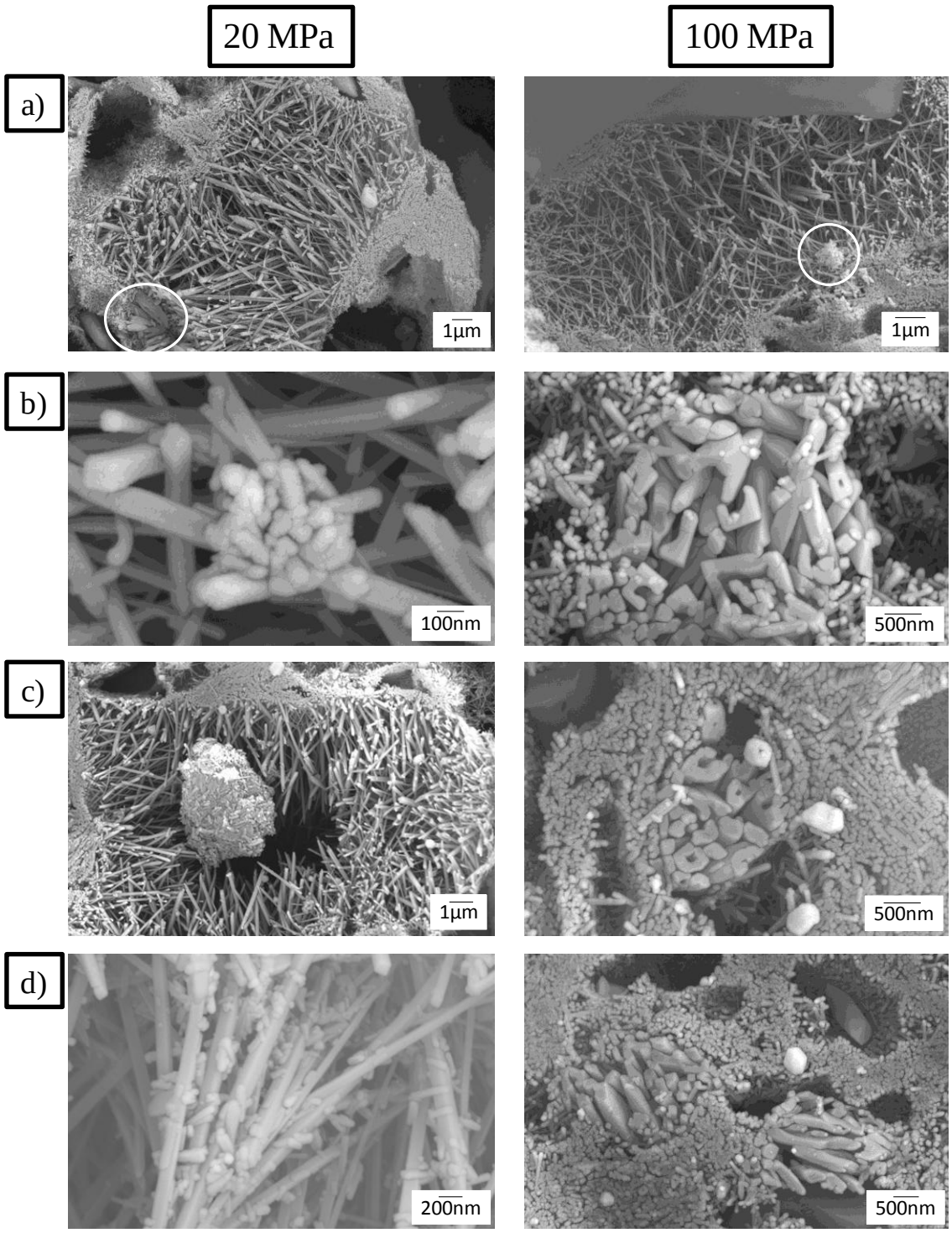

Figure 14. SEM micrograph of fired porcelain stoneware tiles shaped at 20 and 100 MPa with thicknesses of a) 3 mm; b) 4.5 mm; c) 6 mm; d) 9 mm. Circles in a) are provided for guidance.

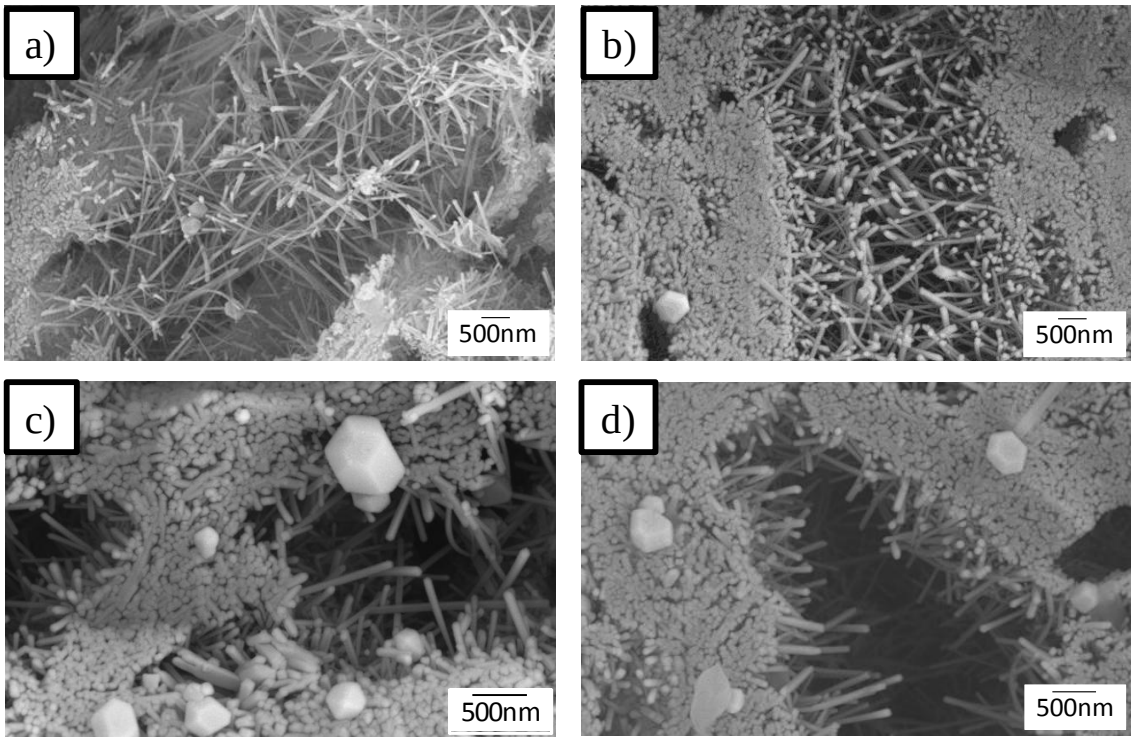

Figure 15. SEM micrograph of tiles moulded at a) 3 mm at 60 MPa, b) 4.5 mm at 100 MPa, c) 6 mm at 100 MPa and d) 9 mm at 60 MPa.

4. Conclusions

A study of the influence of moulding pressure on microstructure and properties of unfired and fired stoneware porcelain tiles has been performed. A mixture of kaolinitic clay (50%), feldspar (40%) and quartz (10%) was selected for the analysis. Five moulding pressures (20, 40, 60, 80 and 100 MPa) and four thicknesses (3, 4.5, 6 and 9 mm) were employed to obtain the unfired tiles, which were fired through a fast-firing process. It can be concluded that as moulding pressure increases the compacting degree (bulk density) of unfired samples, which are almost unaffected at the highest moulding pressures, also increases. Lower shaping pressures have a critical effect on the LS of thinner tiles, and the greatest variations in shrinkage occurred in the fired samples pressed from 20 to 60 MPa. However, this difference is almost negligible in bodies pressed from 60 to 100 MPa.

Technological properties are independent of the thickness of the tiles except for the load of rupture, which is dependent on the thickness of tiles and the shape of pores, as higher

resistances are exhibited by tiles with the highest number of lower-sized pores. Moulding pressure distinctly affects the remaining technological properties (water absorption, porosity and bending strength) in the 20–60 MPa range. Higher pressure values have demonstrated a negligible effect on the technological properties of fired tiles.

The microstructure of the fired samples indicates that although pore-size distribution varies with thickness, it is independent of porosity volume. New types of mullite cluster formed regardless of the moulding pressure and thickness. The aspect ratio of Type II mullite crystals is one of the parameters that influenced the bending strength of the tiles.

Acknowledgements

The authors would like to acknowledge Ms. P. Díaz (CSIC) for her technical support of the experiment. J.M. Pérez acknowledges CSIC for their financial support under contract JAEDoc_08_00362.

References

[1] C. Leonelli, F. Bondioli, P. Veronesi, M. Romagnoli, T. Manfredini, G.C. Pellacani, V. Cannillo, Enhancing the mechanical properties of porcelain stoneware tiles: a microstructural approach, J. Eur. Ceram. Soc. 21 (2001) 785-793.

[2] E. Sánchez, M.J. Orts, J. García-Tena, V. Cantavella, Porcelain tile composition effect on phase formation and end products, Am. Ceram. Soc. Bull. 80 (2001) 43-49.

[3] M. Dondi, G. Guarini, C. Melandri, M. Raimondo, P.M.T. Cavalante, C. Zanelli, Resistance to deep abrasion of porcelain stoneware tiles, Ind. Ceram. 25 (2005) 71-78.

[4] M. Romero, J. Martín-Márquez, J.Ma. Rincón, Kinetic of mullite formation from a porcelain stoneware body for tiles production, J. Eur. Ceram. Soc. 26 (2006) 1647-1652.

[5] J.M. Amigó, J.V. Clausell, V. Esteve, J.M. Delgado, M.M. Reventós, L.E. Ochando, X-Ray powder diffraction phase analysis and thermomechanical properties of silica and alumina porcelains, J. Eur. Ceram. Soc. 24 (2004) 75-81.

[6] S.L. Correia, A.P.N. Oliveira, D. Hotza, A.M. Segadães, Properties of triaxial porcelain bodies: interpretation of statistical modelling, J. Am. Ceram. Soc. 89 (2006) 3356-3365.

[7] Y. Iqbal, W.E. Lee, Fired porcelain microstructure revisited, J. Am. Ceram. Soc. 82 (1999) 3584-3590.

[8] J.M. Perez, J.Ma. Rincon, M. Romero, Effect of moulding pressure on microstructure and technological properties of porcelain stoneware, Ceram. Int. 38 (2012) 317-325.

[9] M.F. Abadir, E.H. Sallam, I.M. Bakr, Preparation of porcelain tiles from Egyptian raw materials, Ceram. Int. 28 (2002) 303-310.

[10] E. Bernardo, M. De Lazzari, P. Colombo, A.S. Llaudis, F.J. Garcia-Ten, Lightweight Porcelain Stoneware by Engineered CeO_2 Addition, Adv. Eng. Mat. 12 (2010) 65-70.

[11] J. García-Ten, A. Saburit, E. Bernardo, P. Colombo, Development of lightweight porcelain stoneware tiles using foaming agents, J. Eur. Ceram. Soc. 32 (2012) 745-752.

[12] U. Morselli, Plastic state shaping with variable thicknesses, Ceramic World Review, 83 (2009) 96-100.

[13] V. Cantavella, J. Garcia-Ten, E. Sanchez, E. Bannier, J. Sanchez, C. Soler, J. Sales, Delayed curvatures in porcelain tiles–Analysis and measurements of influencing factors, CFI-Ceram. Forum Int. 85 (2008) 50-58.

[14] M. Raimondo, M. Dondi, C. Zanelli, G. Guarini, A. Gozzi, F. Marani, L. Fossa, Processing and properties of large/sized ceramic slabs, Bol. Soc. Esp. Ceram. V. 49 (2010) 289-296.

[15] J. Martín-Márquez, J.Ma. Rincón, M. Romero, Effect of firing temperature on sintering of porcelain stoneware tiles, Ceram. Int. 34 (2008) 1867-1873.

[16] W.G. Fahrenholtz, Clays, in: J.F. Shackelford, R.H. Doremus (Eds.), Ceramic and Glass Materials, Structure, Properties and Processing, Springer, New York, 2008, pp. 111-135.

[17] J.L. Amorós, A operação de prensagem: Considerações técnicas e sua aplicação industrial. Parte II: A compactação, Ceram. Industr. 5 (2000) 14-20.

[18] J. L. Amorós, M.J. Orts, J. Garcia-Ten, A. Gozalbo, E. Sanchez, Effect of the green porous texture on porcelain tile properties, J. Eur. Ceram. Soc., 27 (2007)2295-2301.

[19] A. Salem, S.H. Jazayeri, A. Tucci, G. Timellini, Influence of firing temperature, soaking time on sintering of porcelain stoneware tiles, CFI-Ceram. Forum Int. 80 (2003) E66-E70.

[20] C. Zanelli, M. Raimongo, M. Dondi, G. Guarini, P.M. Tenorio Cavalcante, Mecanismos de sinterización de piezas de gres porcelánico, Ceram. Inf. 312 (2004) 57-66.

[21] J. Ranogajec, M. Djuric, M. Radeka, P. Jovanic, Influence of particle size and furnace atmosphere on the sintering of powder for tiles production, Ceram. Silik. 44 (2000) 71-77.

[22] A. Salem, S.H. Jazayeri, E. Rastelli, G. Timellini, Kinetic model for isothermal sintering of porcelain stoneware body in presence of nepheline syenite, Thermochim. Acta 503-504 (2010) 1-7.

[23] P.M.T Cavalcante, M. Dondi, G. Ercolani, G. Guarini,C. Melandri, M. Raimondo, E.R. Almendra, The influence of microstructure on the performance of white porcelain stoneware, Ceram. Int. 30 (2004) 953-63.

[24] M. Dondi, G. Ercolani, C. MelandriC, C. Mingazzini, M. Marsigli, The chemical composition of porcelain stoneware tiles and its influence on microstructural and mechanical properties, Interceram 48 (1999) 75-83.

[25] L. Carbajal, F. Rubio-Marcos, M.A. Bengochea, J.F. Fernández JF, Properties related phase evolution in porcelain ceramics, J. Eur. Ceram. Soc. 27 (2007) 5-9.

[26] C. Gil, M.C. Peiró, J.J. Gómez, L. Chiva, E. Cerisuelo, J.B. Carda, Study of porosity in porcelain tile bodies, Proc. Qualicer (2006) 43-48.

[27] J.L. Amorós, A Operação de Prensagem: Considerações técnicas e sua aplicação industrial. Parte III: Variáveis do processo de compactação, Ceram. Industr. 6 (2001) 15-23.

[28] J.L. Amorós, A Operação de Prensagem: Considerações técnicas e sua aplicação industrial. Parte I: O Preenchimento das cavidades do molde, Ceram. Industri. 5 (2000) 23-28.

[29] T.K. Mukhopadhyay, S. Ghatak, H.S. Maiti, Effect of pyrophyllite on the mullitization in triaxial porcelain system, Ceram. Int. 35 (2009) 1493-1500.

[30] S.R. Bragança, C.P. Bergmann, A view of whitewares mechanical strength and microstructure, Ceram. Int. 29 (7) (2003) 801-806.

[31] J. Martín-Márquez, J.Ma. Rincón, M. Romero, "Effect of microstructure on mechanical properties of porcelain stoneware, J. Eur. Ceram. Soc. 30 (15) (2010) 3063-3069.

[32] J. Martin-Marquez, A.G. De la Torre, M.A.G. Aranda, J.Ma. Rincón, M. Romero, Evolution with temperature of crystalline and amorphous phases in porcelain stoneware, J. Am. Ceram. Soc. 92 (2009) 229-234.

[33] Y. Iqbal, E.J. Lee, Microstructural evolution in triaxial porcelain, J. Am. Ceram. Soc. 83 (2000) 3121–3127.

[34] E. Sánchez, J. García-Ten, M. J. Ibáñez, C. Feliu, J. Sánchez, J. Portolés, Estudio comparativo de propiedades de piezas de gres porcelánico pulido, Ceram. Inf. 314 (2004) 56-66.

[35] C. Zanelli, M. Raimondo, G.Guarini, M. Dondi, The vitreous phase of porcelain stoneware: Composition and evolution during sintering and physical properties, J. Non-Cryst. Solids 357 (2011) 3251-3260.

[36] A. de Noni Jr, D. Hotza, V. Cantavella, E. Sánchez, Influence of composition on mechanical behaviour of porcelain tile. Part III: Effect of the cooling rate of the firing cycle, Mater. Sci. Eng. A-Struct. Mater. Prop. Microstruct. Process. 528 (2011) 3330-3336.

[37] J. Martín-Márquez, J.Ma. Rincón, M. Romero, Mullite development on firing in porcelain stoneware bodies, J. Eur. Ceram. Soc. 30 (2010) 1599-1607.